STATIC AND DYNAMIC EFECTIVE THICKNESS IN MULTILAYERED GLASS PLATES

M. López-Aenlle[a*], F. Pelayo[a]

[a]Department of Construction and Manufacturing Engineering, University of Oviedo, Campus de Gijón, Zona Oeste, Edificio 7, 33203, Gijón, Spain.

[*]corresponding author; E-mail: aenlle@uniovi.es
Phone: +34985 182057

Abstract.

In the last years, the effective thickness concept has been used to calculate deflections, stresses and modal parameters in laminated glass beams and plates, which consists of using a monolithic model with equivalent bending properties to a laminated element, i.e. the thickness of the equivalent monolithic model is time and temperature dependent. Multi-layered laminated glass panels are those with at least three monolithic glass layers and two viscoelastic interlayers which are commonly used in floors, roofs and other applications where a high level of security is required. In this paper, a static deflection effective stiffness for a laminated glass plate consisting of three glass layers and two polymeric interlayers is derived. This static effective thickness is then extended to the frequency domain using the correspondence principle. The models are validated by static experimental tests and operational modal tests carried out on a rectangular multi-layered laminated glass plate pinned supported at the four corners.

Keywords: A. Laminated glass ; B. Operational Modal Analysis ; C. Effective Thickness; D. Viscoelasticity.

NOMENCLATURE

$A_i = bH_i$

D	Flexural Stiffness in plates
E	Young modulus
EI^*	Complex flexural stiffness in beams
EI	Flexural stiffness in beams
$G_2(t,T)$	Viscoelastic relaxation shear modulus for the polymeric interlayer
$G_2^*(\omega,T)$	Complex shear modulus for the polymeric interlayer
H_i	Thickness of glass layer 'i' in laminated glass
I	Second moment of area
$I_i = \dfrac{bH_i^3}{12}$	Second moment of area of glass layer 'i'
L	Length of a glass beam
T	Temperature

LOWERCASE LETTERS

a	Dimension of a plate
b	Dimension of a plate
a_T	Shift factor

b	Width of a glass beam
$g(x)$	Shape function in beams
$g(x,y)$	Shape function in plates
i	Imaginary unit
k_I	Wavenumber
k_M^*	Complex wavenumber
t	Time
t	Thickness of the interlayer
t_i	Thickness of the interlayer 'i'
w	Deflection

GREEK LETTERS

ζ	Modal damping ratio
η	Loss factor
ν	Poisson ratio of layer
ρ_G	Mass density of glass
ρ_t	Mass density of the interlayer
ω	Frequency

1 INTRODUCTION

The simplest laminated glass panel consist of two outer monolithic glass layers and one interlayer of a polymer which usually exhibits a viscoelastic behavior (Figure 1). Multi-layered laminated glass panels (Figure 1) are those with at least three monolithic glass layers and two interlayers [1, 2]. Glass mechanical behavior is usually modeled as linear-elastic whereas the mechanical behavior of polymeric interlayers is commonly assumed as linear-viscoelastic. With these assumptions, laminated glass elements exhibit a linear-viscoelastic behavior, i.e. the response of laminated glass elements is time (or frequency) and temperature dependent [3, 4, 5, 6]. Due to the shear effect of the interlayers, the sections do not behave according to the Euler-Bernoulli Beam theory assumptions, i.e. plane sections do not remain plane [7, 8].

Multi-layered laminated glass plates are commonly used in floors, roofs, other horizontal glazing accessible to the public [9], glass walkways [10], security glass, blast resistant glass, ballistic resistant glass, etc. Moreover, multi-layered laminated glass panels are mandatory in some codes and standards [11, 12].
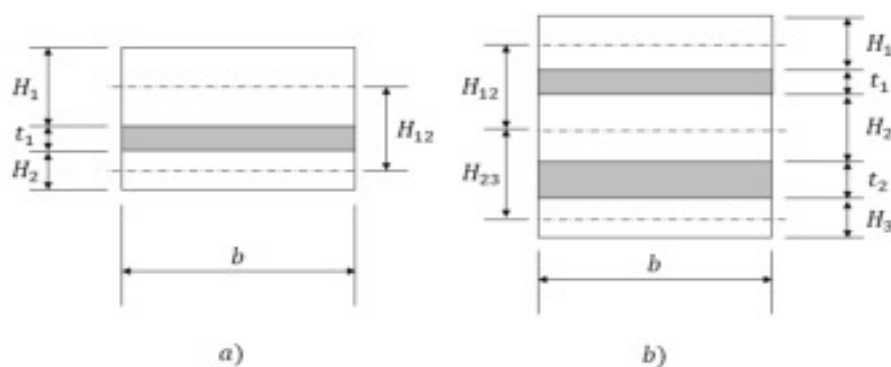

Figure 1. Section of a sandwich (a) and a multi-layered (b) glass beam.

Some analytical models were proposed in the past to predict the modal parameters of sandwich beams with viscoelastic core [13, 14, 15, 16, 17, 18, 19]. Ross, Kerwin and Ungar (RKU) were the first to study the flexural vibration of a sandwich configuration

[13, 14] and they proposed an effective complex flexural stiffness which can be used to determine the modal parameters of a sandwich beam using the equations and the wavenumbers corresponding to an Euler-Bernoulli beam. They assumed that the wave motion in a constrained layer configuration can be described by a fourth-order differential equation. Ditaranto [15, 16] and Mead and Markus [17, 18] demonstrated that the flexural motion of a sandwich beam is governed by a sixth-order linear homogeneous differential equation. Aenlle and Pelayo [20] proposed a dynamic effective thickness for calculating modal parameters in laminated glass beams using simple monolithic elastic models.

With respect to the modal parameters of laminated glass plates, Wang [21] derived an exact relationship between the natural frequencies of a simply supported rectangular sandwich plate and those corresponding to a monolithic Kirchhoff plate with the same geometry and boundary conditions. Modification factors can be used in the formulas to consider other boundary conditions. Nashif et al. [22] proposed to extend the RKU model for beams to the two dimensional case of rectangular laminated glass plates.

Mead [23] and Mead and Yaman [24] proposed a model to predict the vibration response of a rectangular sandwich plate, consisting of two glass layers with same thickness and one viscoelastic interlayer, subject to a harmonic line force which varies sinusoidally across the plate. Aenlle and Pelayo [25] derived a dynamic effective stiffness to calculated modal parameters in laminated glass plates using the analytical equations existing for monolithic plates.

Galuppi and Royer-Carfagni [1] developed a model to calculate the static response of a multilayered laminated glass beams with three glass layers and two polymeric interlayers. Pelayo and Aenlle [26], applying the correspondence principle to the static stiffness obtained from the Galuppi and Royer Carfagni model [1], derived a dynamic effective stiffness which was used to predict the modal parameters of a multilayered glass beam.

In this paper, the static effective stiffness of a rectangular laminated glass plate with three glass layers and two polymeric interlayers is formulated and validated by a static test with a concentrated load at the mid-point. Then, the static effective stiffness is then extended to the frequency domain using the correspondence principle [20, 25, 26]. In order to

validate the model, the modal parameters of a laminated glass plate consisting of three annealed glass layers and two PVB interlayers, pinned supported at the corners, were estimated by operational modal analysis at 20 ºC. The experimental results are compared with the predictions provided by the proposed analytical model.

2 STATE OF THE ART IN BEAMS

2.1 Laminated glass beam with two glass layers and one interlayer.

2.1.1 Mead and Markus Model

Mead and Markus [17, 18] derived a sixth-order differential equation that governs the flexural wave motion of a three layered constrained-layer damping beam when it vibrates freely at frequency ω, which particularized for a laminated glass beam, it is given by:

$$EI_{T2}\left(w^{VI}(x,t) - g_{B2}^*(\omega,T)\left(1 + Y_{B2}\right)w^{IV}(x,t)\right) - \omega^{*2}\,\overline{m}_2 L^4\left(w^{II}(x,t) - g_{B2}^*(\omega,T)\,w(x,t)\right) = 0 \tag{1}$$

where

- subindex "2" indicates beam with two glass layers and one interlayer

- $\omega^{*2} = \omega^2(1 + i\cdot\eta)$ is the complex natural frequency

- $I_{T2} = I_1 + I_2 = b\dfrac{H_1^3 + H_2^3}{12}$ \hfill (2)
- $I_{TOT2} = I_{T2} + A_1 d_1^2 + A_2 d_2^2$ \hfill (3)

- Y_{B2} is a dimensionless geometric parameter given by:

- $Y_{B2} = \dfrac{EI_{TOT2}}{EI_{T2}} - 1 = \dfrac{\left(A_1 d_1^2 + A_2 d_2^2\right)}{I_{T2}} = \dfrac{bH_{12}^2 H_1 H_2}{I_{T2}(H_1 + H_2)}$ \hfill (4)

- $d_i\ (i = 1,2)$ is the distance of the mid-plane of the i-th glass layer from the mid-plane of the whole laminated glass beam, given by:

- $d_1 = \dfrac{H_2 H_{12}}{H_1 + H_2}$ \hfill (5)
- $d_2 = -\dfrac{H_1 H_{12}}{H_1 + H_2}$ \hfill (6)

- $H_{12} = t + \left(\dfrac{H_1 + H_2}{2}\right) = d_1 - d_2$ (7)

- $\overline{m_2}$ is the mass per unit area i.e.:

- $\overline{m_2} = b\rho_G(H_1 + H_2) + b\rho_t t$ (8)

- $g_{B2}^*(\omega)$ is a non-dimensional shear parameter [17, 18], commonly used in sandwich beams, given by:

- $g_{B2}^*(\omega,T) = \dfrac{G_t^*(\omega,T)H_{12}^2}{E} \dfrac{bL^2}{t\ I_{T2}Y_{B2}} = \dfrac{G_t^*(\omega,T)}{E}\dfrac{(H_1 + H_2)L^2}{tH_1H_2}$ (9)

- $G_t^*(\omega,T)$ is the complex shear modulus.

Eq. (1) yields the following polynomial equation:

$$EI_{T2}\left[(k_M^*L)^6 - g_{B2}^*(\omega)(1 + Y_{B2})(k_M^*L)^4\right] - \overline{m_2}\omega^{*\,2}L^4(k_M^*L)^2 + \omega^{*\,2}\overline{m_2}L^4 g_{B2}^*(\omega) = 0 \quad (10)$$

Where $k_M^* = k_R + i \cdot k_I$ is the complex wavenumber.

Eq. (10) can also be expressed as:

$$\omega^2(1 + i \cdot \eta) = \dfrac{k_M^{*\,4}}{\overline{m_2}}EI_{T2}\left(1 + \dfrac{Y_{B2}}{1 - \dfrac{L^2\,k_M^{*\,2}}{g_{B2}^*(\omega)}}\right) \quad (11)$$

If the real part of k_M^* is neglected, i.e., $k_R = 0$, k_M^{*} is given by $k_M^* = i \cdot k_I$ and Eq. (11) results in:

$$\omega^2(1 + i \cdot \eta) = \dfrac{k_I^4}{\overline{m_2}}EI_{T2}\left(1 + \dfrac{Y_{B2}}{1 + \dfrac{L^2k_I^2}{g_{B2}^*(\omega)}}\right) \quad (12)$$

If Eq. (12) is expressed in the same manner as in linear-elastic monolithic beams [28], i.e.:

$$\omega^{*2} = \omega^2(1 + i \cdot \eta) = k_I^4 \frac{EI^*(\omega,T)_2}{\overline{m}_2}$$ (13)

The following expression for the flexural stiffness of the laminated glass beam is derived:

$$EI^*(\omega,T)_2 = EI_{T2}\left(1 + \frac{Y_{B2}}{1 + \frac{L^2 k_I^2}{g_{B2}^*(\omega)}}\right) = EI_{T2}\left(1 + \frac{Y_{B2}}{1 + \frac{EH_1 H_2 t}{G_t^*(\omega)(H_1 + H_2)}k_I^2}\right)$$ (14)

2.1.2 Static deflection effective thickness

Galuppi and Royer-Carfagni [8] derived an analytical expression for the static deflection of a laminated glass beam composed of two glass layers and one polymeric interlayer. The authors assume that the deflection shape of the laminated glass beam coincide with that of a monolithic beam with the same loading and boundary conditions, i.e., the deflection $w(x,t,T)$ of the beam is expressed as:

$$w(x,t,T) = \frac{g(x)}{EI(t,T)_{S2}}$$ (15)

where g(x) is a shape function that takes the form of the elastic deflection of a monolithic beam with constant cross section under the same loading and boundary conditions as the laminated glass beam and $EI(t,T)_{S2}$ is the bending stiffness of the laminated glass beam, which can be expressed as:

$$EI(t,T)_{S2} = EI_{T2}\left(1 + \frac{Y_{B2}}{1 + \frac{\psi_{B2} L^2}{g_{B2}(t,T)}}\right)$$ (16)

where

- ψ_{B2} is a constant parameter which depends on the boundary and loading conditions [2] and it is given by:

$$\psi_{B2} = \frac{\int_0^L (g''(x))^2 \, dx}{\int_0^L (g'(x))^2 \, dx} \tag{17}$$

- $g_{2B}(t,T)$ is a dimensionless shear parameter given by:

$$g_{B2}(t,T) = \frac{G_t(t,T)L^2(H_1 + H_2)}{EtH_1H_2} = \frac{G_t(t,T)H_{12}^2}{E} \frac{bL^2}{t \, I_{T2}Y_{B2}} \tag{18}$$

- $G_t(t,T)$ is the shear modulus of the interlayer

If the shear modulus is constant $G_t(t,T) = G_t$, the shear parameter is also constant i.e.:

$$g_{BE2} = \frac{G_t L^2(H_1 + H_2)}{EtH_1H_2} = \frac{G_t H_{12}^2}{E} \frac{bL^2}{t \, I_{T2}Y_{B2}} \tag{19}$$

If Eq. (19) is substituted in Eq. (16), the later becomes:

$$EI_{E2} = EI_{T2}\left(1 + \frac{Y_{B2}}{1 + \frac{\psi_B L^2}{g_{BE2}}}\right) \tag{20}$$

Which is also constant and it represents the stiffness of the sandwich beam when both the core and the glass layers show a linear-elastic behavior.

2.1.3 Dynamic effective thickness by the correspondence principle

The correspondence principle [3, 4] states that if a solution to a linear elasticity problem is known, the solution to the corresponding problem for a linearly viscoelastic material can be obtained by replacing each quantity which can depend on time by its Fourier Transform. In order to apply the correspondence principle, an elasticity solution must be known [6]. Wherever an elastic constant appears, it is replaced with the corresponding complex dynamic viscoelastic function.

For a laminated glass beam with two glass layers and one polymeric interlayer, the effective complex flexural stiffness can be derived applying the correspondence principle to Eq. (20), i.e.:

$$EI(\omega,T)_2 = EI_{T2}\left(1 + \frac{Y_{B2}}{1 + \frac{k_I^2\ L^2}{g_{B2}^*(\omega,T)}}\right) \tag{21}$$

Where the wavenumber k_I^2 plays in dynamics the same role as the parameter ψ_{B2} in statics, as it was demonstrated in [25].

With respect to parameter $g_{B2}^*(\omega,T)$, it can also be derived from Eq. (19) applying the correspondence principle:

$$g_{B2}^*(\omega,T) = \frac{G_t^*(\omega,T)L^2(H_1 + H_2)}{EtH_1H_2} = \frac{G_t(\omega,T)}{E}\frac{H_{12}^2}{t}\frac{bL^2}{I_{T2}Y_{B2}} \tag{22}$$

It can be observed that the complex effective stiffness $EI(\omega,T)_2$ and the shear parameter $g_{B2}^*(t,T)$ derived with the correspondence principle (Eqs. (21) and (22), respectively) coincide with those of the Mead and Markus model, i.e., the same solution is obtained.

The natural frequencies and damping ratios can now be estimated with Eq. (13).

2.2 Static deflection effective thickness in multilayered laminated glass beams

In the case of three glass layers of thicknesses H_1, H_2 and H_3 and two polymeric interlayers with thicknesses t_1 and t_2, the following expression for the static flexural stiffness can also be derived from the model proposed by Galuppi and Royer-Carfagni [1]:

$$EI(t,T)_{S3} = EI_{T3}\left(1 + \frac{Y_{B3}}{1 + \frac{\psi_{B3}L^2}{g_{B3}(t,T)}}\right) \tag{23}$$

Where:

- subindex "3" indicates beam with 3 glass layers

- $I_{T3} = I_1 + I_2 + I_3 = b\frac{H_1^3 + H_2^3 + H_2^3}{12}$ \hfill (24)

- $Y_{B3} = \frac{(A_1 d_1^2 + A_2 d_2^2 + A_3 d_3^2)}{I_{T3}}$ \hfill (25)

- $d_1 = \frac{H_2 H_{12} + H_3(H_{12} + H_{23})}{H_1 + H_2 + H_3}$ \hfill (26)

- $d_2 = d_1 - H_{12}$ \hfill (27)

- $d_3 = d_1 - (H_{12} + H_{23})$ \hfill (28)

- $H_{12} = t_1 + \left(\frac{H_1 + H_2}{2}\right) = d_1 - d_2$ \hfill (29)

- $H_{23} = t_2 += d_2 - d_3$ \hfill (30)

- $g_{B3}(t,T) = \frac{G_t(t,T)b\left(\frac{H_{12}^2}{t_1} + \frac{H_{23}^2}{t_2}\right)L\char`\^2}{E\, I_{T3}Y_{B3}}$ \hfill (31)

- $\psi_{B3} = \psi_{B2}$ is a constant parameter which takes the same values as those derived for a beam with 2 glass layers [8].

It can be verified that the effective stiffness $EI(t,T)_{S2}$ and the shear parameter $g_{B2}(t,T)$ corresponding to the case with two glass layers can be derived from Eqs. (23) and (31), respectively, taking $H_3 = 0$, $t_2 = 0$, $H_{23} = 0$ and $d_3 = 0$

If the shear modulus is constant $G_t(t,T) = G_t$, the elastic shear parameter is given by:

$$g_{BE3} = \frac{G_t b \left(\dfrac{H_{12}^2}{t_1} + \dfrac{H_{23}^2}{t_2} \right) L^2}{E \, I_{T3} Y_{B3}} \tag{32}$$

Whereas the elastic flexural stiffness is expressed as:

$$EI_{E3} = EI_{T3} \left(1 + \frac{Y_{B3}}{1 + \dfrac{\psi_{B3} L^2}{g_{BE3}}} \right) \tag{33}$$

2.2.1 Dynamic effective thickness by the correspondence principle

Applying the correspondence principle to Eq. (13), the following expression for the complex effective thickness is derived:

$$EI(\omega,T)_3 = EI_{T3} \left(1 + \frac{Y_{B3}}{1 + \dfrac{k_I^2 \, L^2}{g_{B3}^*(\omega,T)}} \right) \tag{34}$$

With respect to parameter $g_{B3}^*(\omega,T)$, applying the correspondence principle to Eq. (31) the following expression is obtained:

$$g_{B3}^{*}(\omega,T) = \frac{G_t(\omega,T)b\left(\dfrac{H_{12}^2}{t_1} + \dfrac{H_{23}^2}{t_2}\right)L^2}{E\,I_{T3}Y_{B3}} \tag{35}$$

The natural frequencies and damping ratios can be calculated with:

$$\omega^2(1 + i \cdot \eta) = \frac{k_I^4}{\overline{m}_3}EI^*(\omega,T)_3 \tag{36}$$

where:

$$\overline{m}_3 = 3b\rho_G H + 2\rho_t bt \tag{37}$$

is the mass per unit length of the beam.

3 STATE OF THE ART IN PLATES

3.1 Laminated glass plates with two glass layers and one interlayer.

3.1.1 Mead and Yaman Model

Mead [23] and Mead and Yaman [24] derived a sixth-order differential equation that governs the flexural wave motion of a symmetric ($H = H_1 = H_2$) rectangular constrained-layer sandwich plate, which particularized for a laminated glass plate yields the following characteristic equation:

$$D_{T2}\left[\left(k_M^* a\right)^6 - g_{MY}^*(\omega,T)(1 + Y_{MY})\left(k_M^* a\right)^4\right] - \omega^{*2}(\rho H)_2 a^4 \left(k_M^* a\right)^2 + \omega^{*2} a^4 (\rho H)_2 g_{MY}^*(\omega,T) = 0 \tag{38}$$

where:

- $k_M^* = k_R + i \cdot k_I$ is the complex wavenumber.
- Y_{MY} is a dimensionless geometric parameter given by:

$$Y_{MY} = 3\left(1 + \frac{t}{H}\right)^2 \tag{39}$$

- g_{MY}^* is a dimensionless shear parameter commonly used in sandwich plates [23, 24] which defines the shear coupling between the core and outer layers:

$$g_{MY}^* = \frac{2G_t(\omega,T)(1-v^2)a^2}{EtH} \tag{40}$$

- $(\rho H)_2 = \rho_G(H_1 + H_2) + \rho_t t \tag{11}$

Eq. (38) can also be expressed as:

$$\omega^2(1 + i \cdot \eta) = \frac{k_M^{*4}D_{T2}}{(\rho H)_2}\left(1 + \frac{Y_{MY}}{1 - \dfrac{k_M^{*2}\,a^2}{g_{MY}^*(\omega,T)}}\right) \tag{42}$$

If the real part of k_M^* is neglected, i.e., $k_R = 0$, k_M^* is given by $k_M^* = i \cdot k_I$ and Eq. (42) results in:

$$\omega^{*2} = \omega^2(1 + i \cdot \eta) = \frac{k_I^4 D_{T2}}{(\rho H)_2}\left(1 + \frac{Y_{MY}}{1 + \dfrac{k_I^2\,a^2}{g_{MY}^*(\omega,T)}}\right) \tag{43}$$

From which the following equation for the effective complex flexural stiffness is formulated:

$$D^*(\omega,T)_{MY} = D_{T2}\left(1 + \frac{Y_{MY}}{1 + \dfrac{k_I^2\,a^2}{g_{MY}^*(\omega,T)}}\right) \tag{44}$$

3.1.2 Static deflection effective thickness

Galuppi and Royer-Carfagni [27] extended the model for beams [8] to the two dimensional case of a rectangular laminated glass plates under uniform pressure with

different boundary configurations at the borders [27]. They considered the deflection of the plate as:

$$w(x,y,t) = \frac{g(x,y)}{D(t)_{S2}}$$

(45)

where g(x,y) is a shape function that takes the form of the elastic deflection of a monolithic plate with constant cross section under the same loading and boundary conditions, $D(t)_{S2}$ is the stiffness of the laminated glass plate given by:

$$\frac{1}{D(t)_{S2}} = \frac{\eta}{D_{T2}(1 + Y_{P2})} + \frac{1 - \eta}{D_{T2}}$$

(46)

where the non-dimensional parameter η, tune the plate response from the layered limit ($\eta = 0$) to the monolithic limit ($\eta = 1$).

The in-plane displacements in the x and y directions are approximated as:

$$u_i(x,y,t) = -\beta \frac{d_i}{D_{T2}(1 + Y_{P2})} g_x'(x,y) \quad i = 1,2$$

(47)

and

$$v_i(x,y,t) = -\beta \frac{d_i}{D_{T2}(1 + Y_{P2})} g_y'(x,y) \quad i = 1,2$$

(48)

Where β is a non-dimensional parameter which tune the in-plane plate response from the layered limit ($\beta = 0$), null in- plane force in the glass layers) to the monolithic limit ($\beta = 1$).

The total strain energy of the system is expressed as [27]:

$$E(w,u_1,u_3,v_1,v_3)$$

$$= \int_\Omega \left\{ \left[\frac{1}{2D(t,T)_{S2}} \frac{D_{T2}}{} + \beta^2 \frac{D_{T2}Y_P}{(1+Y_{P2}^2)} \right] f_1(g(x,y) + \frac{G_t(t,T)H_{12}^2}{t} \right. \tag{49}$$

$$\left. \left[\frac{1}{D(t,T)_{S2}} - \frac{\beta}{D_{T2}(1+Y_{P2})} \right]^2 f_2(g(x,y) + \frac{p(x,y)}{D(t,T)_{S2}} g(x,y) \right\} dxdy$$

or alternatively

$$E(w,u_1,u_3,v_1,v_3)$$

$$= \int_\Omega \left\{ \left[\frac{1}{2D(t,T)_{S2}} \frac{D_{T2}}{} + \beta^2 \frac{D_{T2}Y_P}{(1+Y_{P2}^2)} \right] f_1(g(x,y) + \frac{g_{2P}(t,T)Y_{P2}D_{T2}}{1-v^2} \right. \tag{50}$$

$$\left. \left[\frac{1}{D(t,T)_{S2}} - \frac{\beta}{D_{T2}(1+Y_{P2})} \right]^2 f_2(g(x,y) + \frac{p(x,y)}{D(t,T)_{S2}} g(x,y) \right\} dxdy$$

where:

- subindex "s" indicates static

- subindex "p" indicates plate

- subindex "2" indicates two glass layer

- Y_{P2} is a dimensionless geometric parameter given by:

$$Y_{P2} = \frac{\sum_{i=1}^{2} \left(\frac{12D_i d_i^2}{H_i^2} \right)}{D_{T2}} = \frac{12D_1 D_2 H_{12}^2}{D_{T2}(D_1 H_2^2 + D_2 H_1^2)} = \frac{12H_{12}^2 H_1 H_2}{(H_1^3 H_2^3)(H_1 + H_2)} \tag{51}$$

- $D_{T2} = D_1 + D_2 = \frac{EH_1^3}{12(1-v^2)} + \frac{EH_2^3}{12(1-v^2)}$ \tag{52}

- $f_1(g(x,y)) = \left(\frac{\partial^2 g(x,y)}{\partial x^2} + \frac{\partial^2 g(x,y)}{\partial y^2}\right)^2 - 2(1-v)\left(\frac{\partial^2 g(x,y)\partial^2 g(x,y)}{\partial x^2} - \left(\frac{\partial^2 g(x,y)}{\partial x \partial y}\right)^2\right)$ (53)

- $f_2(g(x,y)) = \left(\frac{\partial g(x,y)}{\partial x}\right)^2 + \left(\frac{\partial g(x,y)}{\partial y}\right)^2$ (54)

- ψ_{P2} is a constant parameter which depends on the boundary and loading conditions [27] and it is given by:

$$\psi_{P2} = \frac{\displaystyle\int_{\Omega} f_1(g(x,y))dxdy}{\displaystyle\int_{\Omega} f_2(g(x,y))dxdy}$$ (55)

- $g_{P2}(t,T)$ is the dimensionless shear parameter which defines the shear coupling between the core and outer layers:

$$g_{P2}(t,T) = \frac{G_t(t,T)\left(D_1 H_2^2 + D_2 H_1^2\right)a^2}{12 D_1 D_2 t} = \frac{G_t(t,T)}{E/(1-v^2)}\frac{(H_1+H_2)a^2}{H_1 H_2 t}$$ (56)

The flexural stiffness $D(t)_{S2}$ is derived minimizing the total strain energy [27] with respect to the non-dimensional parameters η and β, which results in:

$$D(t)_{S2} = D_{T2}\left(1 + \frac{Y_{P2}}{1 + \frac{\psi_{P2}a^2}{g_{P2}(t,T)}}\right)$$ (57)

3.1.3 Dynamic effective thickness by the correspondence principle

Particularizing Eq. (57) for $G_t(t,T) = G_t$ and applying the correspondence principle, the effective complex flexural stiffness for a laminated glass plate with two glass layers and one polymeric interlayers of thickness t, is derived:

$$D^*(\omega,T)_2 = D_{T2}\left(1 + \frac{Y_{P2}}{1 + \frac{k_I^2 \, a^2}{g_{P2}^*(\omega,T)}}\right) \tag{58}$$

Whereas the parameter $g_{P2}^*(\omega,T)$ is expressed as (using the correspondence principle [3, 4, 6]):

$$g_{P2}^*(\omega,,T) = \frac{G_t^*(\omega,T)}{E/(1-v^2)} \frac{(H_1 + H_2)a^2}{H_1 H_2 t} \tag{59}$$

If Eqs. (51), (58) and (59) are particularized for the symmetric case ($H = H_1 = H_2$), it is inferred that $Y_{MY} = Y_{P2}$, $g_{MY}^*(\omega,T) = g_{P2}^*(\omega,T)$ and $D^*(\omega,T)_{MY} = D^*(\omega,T)_2$, i.e., the equations derived with the correspondence principle coincide with those developed by Mead and Yaman [24].

The natural frequencies and the loss factors can be estimated with the expression:

$$\omega^{*2} = \omega^2(1 + i \cdot \eta) = k_I^4 \frac{D^*(\omega,T)_2}{(\rho H)_2} \tag{60}$$

If Eqs. (4) and (51) are compared, it is inferred that $Y_{P2} = Y_{B2}$. Thus, the shear parameters are related by $g_{P2}^*(t,T) = \frac{g_{B2}^*(t,T)}{(1-v^2)}$. If $v = 0$ the complex stiffness of the laminated glass plate coincides with the stiffness of the unit width laminated glass beam ($b = 1$) i.e.:

$$D^*(\omega,T)_2 = EI_{T2} \quad if \ v = 0 \ , \ b = 1 \ and \ a = L \tag{61}$$

4 MULTILAYERED PLATES

4.1 Static deflection effective thickness

Assuming again the deflection of the plate as:

$$w(x,y,t) = \frac{g(x,y)}{D(t,T)_{S3}} \tag{62}$$

Where $g(x,y)$ is a shape function that takes the form of the elastic deflection of a monolithic plate with constant cross section under the same loading and boundary conditions, $D(t,T)_{S3}$ is the flexural stiffness of the plate given by:

$$\frac{1}{D(t)_{S3}} = \frac{\eta}{D_{T3}(1 + Y_{P3})} + \frac{1 - \eta}{D_{T3}} \tag{63}$$

The in-plane displacements in the x and y directions are approximated as:

$$u_i(x,y,t) = -\beta \frac{d_i}{D_{T3}(1 + Y_{P3})} g_x'(x,y) \qquad i = 1,2,3 \tag{64}$$

and

$$v_i(x,y,t) = -\beta \frac{d_i}{D_{T3}(1 + Y_{P3})} g_y'(x,y) \quad i = 1,2,3 \tag{65}$$

where d_i are given by Eqs. (26 to 28). The total strain energy is given by [27]:

$$
\begin{aligned}
\mathrm{E}&(w,u_1,u_2,u_3,v_1,v_2v_3)\\
&= \int_\Omega \left\{ \left[\frac{1}{2D(t,T)_{S3}}\frac{D_{T3}}{} + \beta^2\frac{D_{T3}Y_{P3}}{(1+Y_{P3}^2)}\right] f_1\left(g(x,y) + \frac{G_t(t,T)}{t}\right.\right.\\
&\left.\left[\frac{H_{12}^2}{t_1} + \frac{H_{23}^2}{t_2}\right]\left[\frac{1}{D(t,T)_{S3}} - \frac{\beta}{D_{T3}(1+Y_{P3})}\right]^2 f_2\left(g(x,y) + \frac{p(x,y)}{D(t,T)_{S3}}g(x,y)\right)\right\}\\
&dxdy
\end{aligned}
\tag{66}
$$

or:

$$
\begin{aligned}
\mathrm{E}&(w,u_1,u_3,v_1,v_3)\\
&= \int_\Omega \left\{ \left[\frac{1}{2D(t,T)_{S3}}\frac{D_{T3}}{} + \beta^2\frac{D_{T3}Y_{P3}}{(1+Y_{P3}^2)}\right] f_1\left(g(x,y) + \frac{g_{P3}(t,T)Y_{P3}D_{T3}}{1-v^2}\right.\right.\\
&\left.\left[\frac{1}{D(t,T)_{S3}} - \frac{\beta}{D_{T3}(1+Y_P)}\right]^2 f_2\left(g(x,y) + \frac{p(x,y)}{D(t,T)_{S3}}g(x,y)\right)\right\}dxdy
\end{aligned}
\tag{67}
$$

where:

- subindex "3" indicates three glass layers

- Y_{P3} is a dimensionless geometric parameter given by:

$$
Y_{P3} = \frac{\displaystyle\sum_{i=1}^{3}\frac{12D_id_i^2}{H_i^2}}{D_{T3}}
\tag{68}
$$

- $D_{T3} = D_1 + D_2 + D_3 = \frac{E}{12(1-v^2)}\left(H_1^3 + H_2^3 + H_3^3\right)$ (69)

- $g_{P3}(t,T)$ is the dimensionless shear parameter given by:

$$g_{P3}(t,T) = \frac{G_t(t,T)(1 - v^2)\left[\dfrac{H_{12}^2}{t_1} + \dfrac{H_{23}^2}{t_2}\right]a^2}{Y_{P3}D_{T3}} \tag{70}$$

The flexural stiffness $D(t,T)_{3S}$ is derived minimizing the total strain energy with respect to the non-dimensional parameters η and β, resulting in:

$$D(t,T)_{S3} = D_{T3}\left(1 + \frac{Y_{P3}}{1 + \dfrac{\psi_{P3}a^2}{g_{P3}(t,T)}}\right) \tag{71}$$

where $\psi_{P3} = \psi_{P2}$.

4.2 Dynamic effective thickness by the correspondence principle

Applying the correspondence principle to Eq. (71), the following expression for the effective stiffness is derived:

$$D^*(\omega,T)_3 = D_{T3}\left(1 + \frac{Y_{P3}}{1 + \dfrac{k_I^2 a^2}{g_{P3}^*(\omega,T)}}\right) \tag{72}$$

whereas the parameter $g_{P3}^*(\omega,T)$, it is given by:

$$g_{P3}^*(t,T) = \frac{G_t^*(\omega,T)(1 - v^2)\left[\dfrac{H_{12}^2}{t_1} + \dfrac{H_{23}^2}{t_2}\right]a^2}{Y_{P3}D_{T3}} \tag{73}$$

The natural frequencies and the loss factors can be estimated with the expression

$$\omega^{*2} = \omega^2(1 + i \cdot \eta) = k_I^4 \frac{D^*(\omega,T)_3}{(\rho H)_3} \qquad (74)$$

where $(\rho H)_3$ is the mass per unit area:

$$(\rho H)_3 = \rho_G(H_1 + H_2 + H_3) + \rho_t(t_1 + t_2) \qquad (75)$$

It can be verified that the effective stiffness $D^*(\omega,T)_{S2}$ and the shear parameter $g_{P2}^*(\omega,T)$ corresponding to the case with two glass layers can be derived from Eqs. (73) and (74), respectively, taking $H_3 = 0$, $t_2 = 0$, $H_{23} = 0$ and $d_3 = 0$.

4. EXPERIMENTAL TESTS

4.1 Modal tests

A rectangular laminated glass plate 1400 x 1000 mm and thickness $H_1 = 3.80$ mm, $H_2 = 3.75$ mm, $H_3 = 3.87$ mm and $t_1 = t_2 = 0.76\,mm$, pinned supported at the four corners using four wooden balls with a diameter of 50 mm (see Fig. 2), were tested using operational modal analysis (OMA) [29] at room temperature T $= 20\ ^oC$.
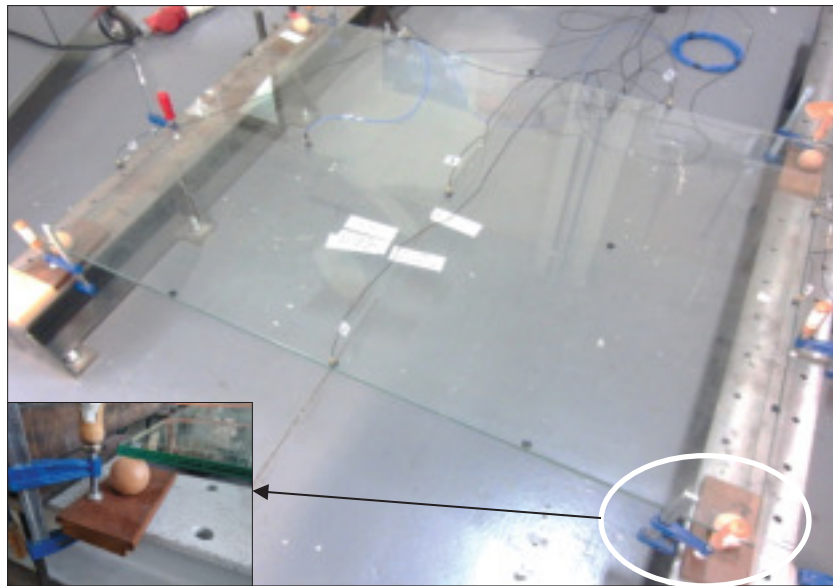
Figure 2. Multilayered glass plate under simply supported conditions.

The plate was excited applying many small hits on the upper plate surface using an impact hammer [30]. The hits were applied randomly in time and space. The responses of the plate were measured in 15 points (see Figure 3) using 8 accelerometers with a sensitivity of 100 mv/g, uniformly distributed along the plate using three different data sets. The responses were recorded for approximately 4 minutes with a sampling frequency of 1000 Hz and using a 8 channel digital acquisition system. The singular value decomposition of the responses is presented in Fig. 4. The spectral densities being calculated using 1024 frequency lines. It is well known that the effect of leakage is always present in the estimation of damping when frequency domain estimation techniques are use unless that long data segments are used. In order to minimize this effect, the responses were decimated by several orders (see Fig. 5). The results presented in Table 2 correspond to the maximum order of decimation that can be used with each mode.
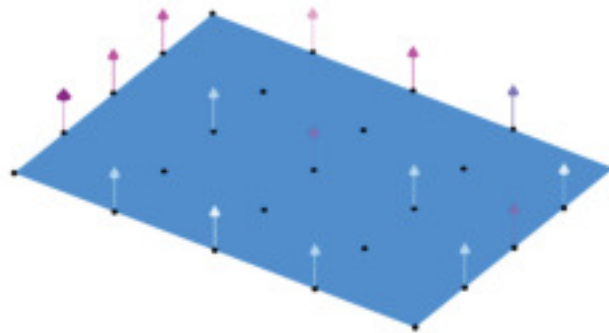
Figure 3. Accelerometers (arrows) Set-up used in the OMA test.

The first 8 modes were identified by OMA and the modal parameters of the plate were estimated using both frequency domain decomposition (EFDD) [29] and the stochastic subspace iteration (SSI) [29] methods, the results being presented in Table 1 (natural frequencies) and Table 2 (damping ratios).
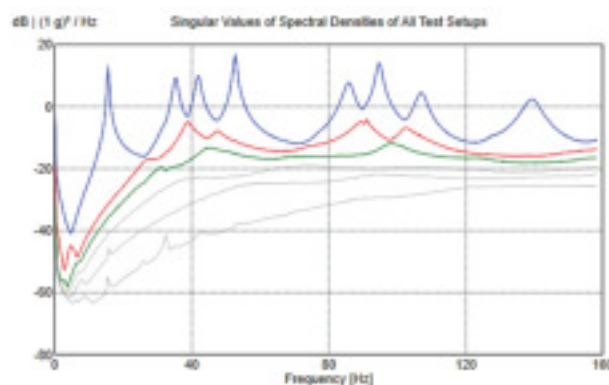
Figure 4. Singular value decomposition of the responses

The modal parameters of the plate were also predicted using Eq. (75). A Young modulus $E = 72000$ MPa, Poisson ratio $\nu = 0.22$ and density $\rho_G = 2500$ kg/m³ were considered for the glass [9]. As regarding the core of the beam, made of polyvinyl butiral (PVB), a density $\rho_t = 1030$ kg/m³ and the complex shear modulus $G_2^*(\omega)$ determined in previous works [25, 26, 31] were considered.

Table 1. Experimental and predicted natural frequencies.

MODE	WAVENUMBER	NATURAL FREQUENCIES [Hz]			ERROR [%]	
		EXPERIMENTAL		PREDICTION Eq. (75)		
		EFDD	SSI		EFDD-Eq. (75)	SSI-Eq. (75)
1	2.2005	15.604	15.607	15.734	0.824	0.805
2	3.4147	35.269	35.279	37.469	5.870	5.844
3	3.6706	41.869	41.812	43.186	3.049	3.181
4	4.1861	52.645	52.643	55.863	5.761	5.765
5	5.3207	85.858	85.721	88.997	3.527	3.681
6	5.6002	94.726	94.721	98.219	3.556	3.561
7	6.0224	107.024	106.956	112.923	5.511	5.578
8	6.8416	139.363	139.276	144.042	3.357	3.422

Table 2. Experimental and predicted damping ratios.

MODE	DAMPING RATIOS [%]			ERROR [%]	
	EXPERIMENTAL		PREDICTION Eq. (75)		
	EFDD	SSI		EFDD- Eq. (75)	SSI- Eq. (75)
1	1.032	0.930	0.967	6.749	3.812
2	1.610	1.715	1.603	0.427	6.977
3	1.719	1.667	1.714	0.300	2.734
4	0.819	0.792	1.921	57.368	58.753
5	1.757	1.698	2.392	26.548	29.015
6	0.818	0.797	2.523	67.579	68.411
7	1.604	1.447	2.735	70.625	70.511
8	1.793	1.829	3.188	77.141	74.302
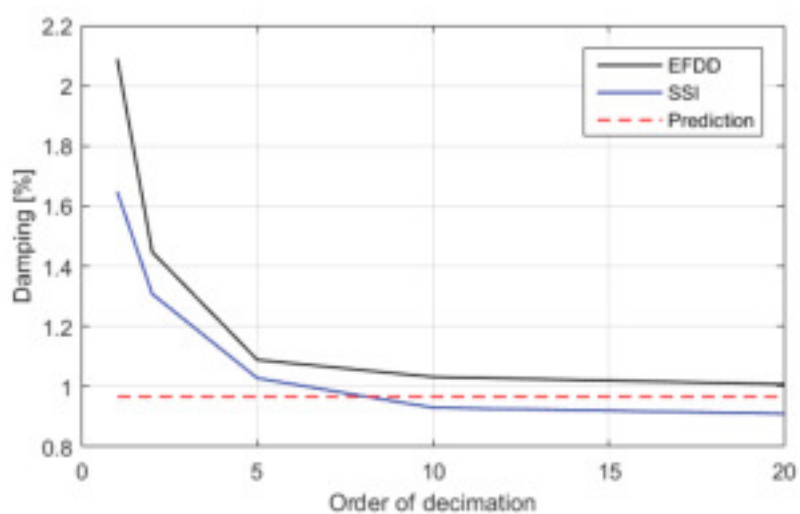
Figure 5. Effect of decimation in the damping estimation for the first mode.

The wavenumbers needed in Eqs. (72) and (74) were estimated using a monolithic FE model with the same dimensions $a = 1400\ mm$, $b = 1000\ mm$, thickness $H = H_1 + H_2 + H_3 + t_1 + t_2 = 12.94\ mm$, pinned supported at the corners and material properties corresponding to the glass (E, ρ_g, v). From the natural frequencies ω_{FEM} of the FE model, the corresponding wavenumbers were obtained using the standard equation of natural frequencies in monolithic plates [28]:

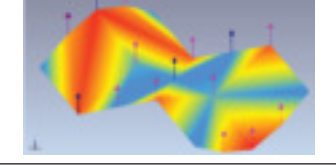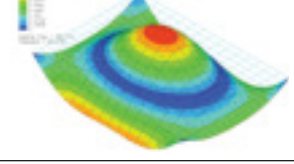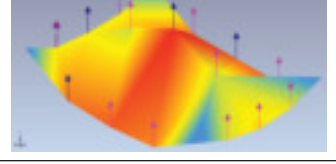$$\omega_{FEM}^2 = k_I^4 \frac{E_1 \frac{H^3}{12}}{(1 - v^2)\rho_G H} \tag{76}$$
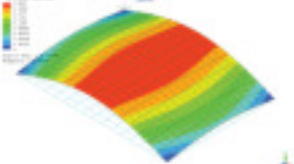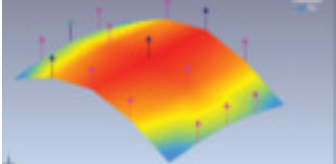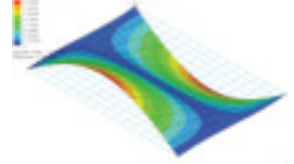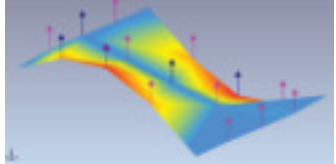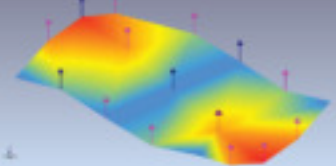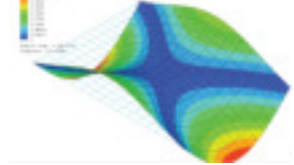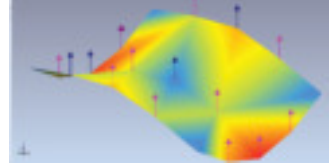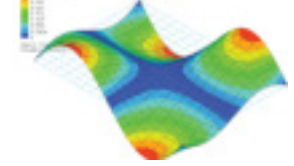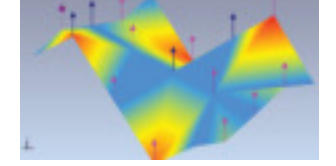
where the only unknowns are the wavenumbers k_I. The estimated wavenumbers are presented in Table 1 together with the experimental and the numerical natural frequencies, whereas the damping ratios are shown in Table 2. It has been considered that loss factor and the modal damping ratio ζ are related by [32]:

$$\eta = 2 \cdot \zeta \tag{77}$$

The experimental and the numerical mode shapes, corresponding to a monolithic plate are shown in Table 3.

It can be observed that the natural frequencies can be estimated with and error less than 6% for all the modes considered in the investigation. With respect to the experimental loss factors, larger discrepancies have been obtained, the maxima error being close to 75% for the higher modes. This large error is expected because in Eqs. (72) and (74) we assume that the real part of the complex wavenumber $k_M^* = k_R + i \cdot k_I$ is $k_R = 0$.

Table 3. Experimental and numerical mode shapes.

MODE	FEM	EXPERIMENTAL
1		
2		
3		
4		
5		
6		
7		

| 8 | | |
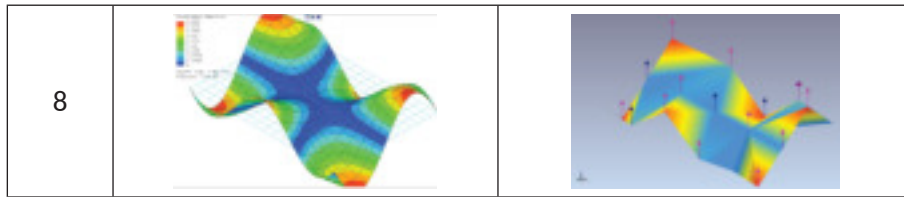
4.1 Static test

The same plate with the same boundary conditions were subject to a constant concentrated static load of 300 N in the mid-point of the plate (Fig. 6). The test was carried out at a temperature of $T = 24^o C$.

The displacements of the beam were measured in two points (A and B in Fig. 6) using two laser sensors. The experimental displacements together with those estimated with Eqs. (62) and (71) are shown in Fig. 7 and 8, from which is inferred that the displacements are predicted with an error less than 14%. Due to the fact that the tests were performed at room temperature for 24 hours, the temperature was not constant but varying from 24.5°C at the beginning of the test to 21.5 °C at the end of the test. The predictions presented in Figure 7 and 8 correspond to a temperature of 24.5 °C which gives the largest error. If both temperatures (24°C and 21.5 °C are plotted (Fig. 7 and 8), it can be observed that the error diminish.
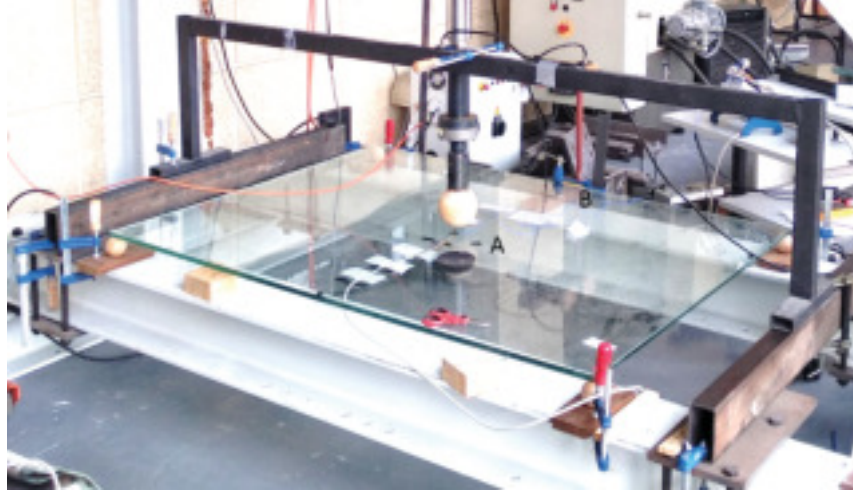
Figure 6. Experimental Set-up for the static test.

With respect to the parameter ψ_{P3} needed in Eq. (71) and corresponding to a rectangular laminated glass plate pinned supported at the four corners and subject to a concentrated loading, it cannot be found in the literature. A finite element model of the plate was assembled in ABAQUS. Shell continuum elements were used for the glass layers whereas 3D Hexaedral elements were used for the viscoelastic core layers [26]. Elastic properties for both glass and PVB (at long term $G_t(t = \infty, T)$) and the stiffness of the plate was obtained from:

$$D(t = \infty, T)_{S3} = \frac{P}{w} \tag{79}$$

Where P is the loading applied at the mid-point of the plate and w the displacement at the same point. Then, the parameter ψ_{P3} was calculated using Eq. (71).
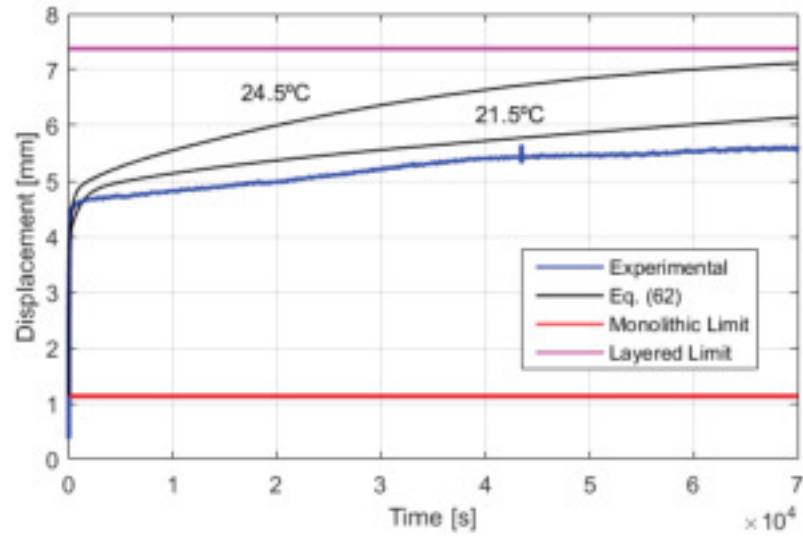
Figure 7. Displacement of the central point of the plate (Point A)
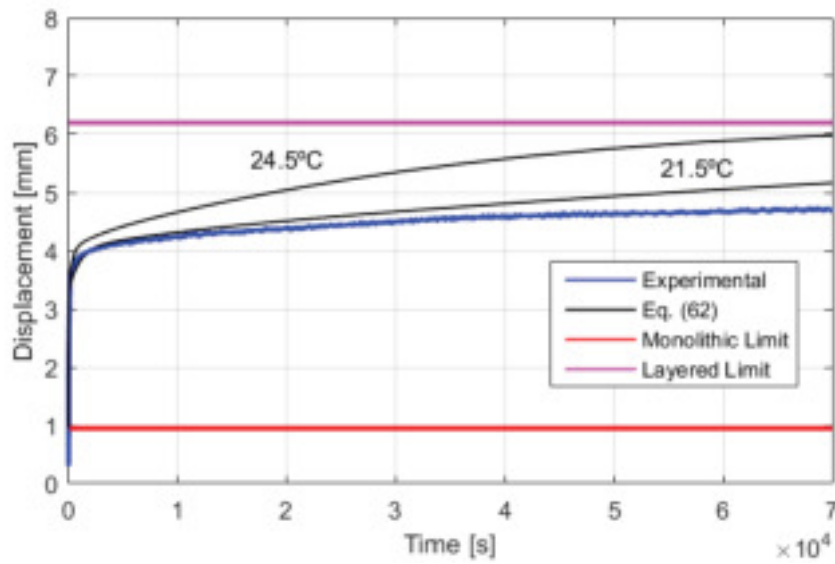

Figure 8. Displacement of the border mid-point (Point B).

5 CONCLUSIONS

Multi-layered laminated glass plates are commonly used in safety and security applications, acoustic isolation, balustrades and floor glazing applications. In the last

years, several papers have been published proposing analytical equations to calculate of stresses, displacements and modal parameters of laminated glass elements consisting of two glass layers and one viscoelastic interlayer, using the effective thickness concept [1, 8, 27] . With this technique the response of laminated glass elements is estimated combining the effective thickness equations with the responses obtained with a monolithic model of the element under the same loading and boundary conditions [1, 8, 27]. With respect to multilayered panels, only equations for multilayered beams have been proposed [1].

In this paper, an analytical expression for the static effective stiffness (from which the effective thickness can easily be derived) of a rectangular laminated glass plate with three glass layers and two viscoelastic polymeric interlayers, has been derived. Then the static effective stiffness has been extended to the dynamic case using the correspondence principle [3, 4, 6].

The analytical expressions developed in this paper have been used to predict the static displacement at room temperature (24.5 ºC) of a multilayered glass plate composed of three glass layers and two polymeric interlayers, pinned supported at the four corners, and subject to a concentrated loading of 300 N for approximately 24 hours and applied at the mid-point of the plate. The parameter ψ_{P3} needed in Eq. (71) has been obtained from the results of a finite element model assembled in ABAQUS. The analytical predictions have been validated with a static test. The results (Figs. 7 and 8) show that the displacements can be predicted with an error less than 14%.

In order to validate the dynamic equations for a multi-layered plate, the natural frequencies and the damping ratios of the same plate and with the same boundary conditions at 20ºC were estimated with Eq. (74). The wavenumbers needed in Eqs. (72) and (74) were obtained from a linear-elastic monolithic finite element model, with the

same dimensions, thickness and boundary conditions. In order to validate the analytical predictions, operational experimental modal tests were carried out on the plate and the modal parameters were estimated by both frequency domain decomposition (EFDD) [29] and the stochastic subspace iteration (SSI) [29] method.

The discrepancies in natural frequencies between the analytical predictions and those estimated with operational modal analysis are less than 6 %. With regard to the damping ratios, the maximum discrepancies between the experimental damping ratios and those predicted with the analytical model are less than 75%. However, these large discrepancies are expected because we assume that the real part of the complex wavenumber $k_M^* = k_R + i \cdot k_I$ is $k_R = 0$. Moreover, it is known from statistical theory that the uncertainty bounds of damping ratios are much higher than those of natural frequencies.

REFERENCES

[1] Galuppi L and Royer-Carfagni GF. Enhanced Effective Thickness of Multi-Layered Laminated Glass. *Compos Part B-Eng* 2014; 64:202-213.

[2] Feldmann M, Kasper R et al. Guidance for European Structural Design of Glass Components. *JCR Scientific and Policy Report*. 2014; doi: 10.2788/5523.

[3] Lee, E.H., Stress Analysis in Viscoelastic Bodies, Q J Mech Appl Math, 1955;13:183-190.

[4] Read, W.T., Stress Analysis for Compressible Viscoelastic Materials. J Appl Phys, 1950;21:671-674.

[5] Ferry, J.D., Viscoelastic Properties of Polymers, Third ed., John Wiley & Sons, Ltd., New York. 1980.[

[6] Lakes, R., Viscoelastic solids. CRC Press, New York, (2009).

[7] Galuppi, L., and Royer-Carfagni, G.F., Laminated Beams with Viscoelastic Interlayer, Int J Solids Struct, 2012;49(18):2637-2645.

[8] Galuppi, L., and Royer-Carfagni, G.F., Effective Thickness of Laminated Glass Beams: New Expression via a Variational Approach, J Struct Eng, 2012;38:53-67.

[9] Haldimann M, Luible A and Overend M. Structural Use of Glass. *Structural Engineering Documents* (10). IABSE, 2008.

[10] Bennison SJ and Surreis F. Designing the Grand Canyon's new laminated glass walkway. In: *Glass Processing Days*, Tampere. Finland, 2007.

[11] ASTM 2751-11. Practice for the Design and Performance of Supported Glass Walkways.

[12] ÖNORM B3716-5. Glass in building – Structural Glass Construction – Part 5: Point fixed Glazing and Special Structures, 2013.

[13] Kerwin, E.M., Damping of Flexural Waves by a Constrained Viscoelastic Layer, J. Acoust. Soc. Am, 1959;31(7):952-962.

[14] Ross, D., Ungar, E.E., and Kerwin, E.M., Damping of Plate Flexural Vibrations by Means of Viscoelastic Laminate, Structural Damping, ASME, 1959; p. 49-88.

[15] DiTaranto, R.A., and McGraw, Jr, J.R., Vibratory Bending of Damped Laminated Plates, J Eng Ind, 1969;91(4):1081-1090.

[16] DiTaranto, R.A., Theory of Vibratory Bending for Elastic and Viscoelastic Layered Finite-Length Beams, J Appl Mech, 1965;32:881-886.

[17] Mead, D.J., and Markus, S., The Forced Vibration of a Three-Layer, Damped Sandwich Beam with Arbitrary Boundary Conditions, J Sound Vib, 1969;10(2):163-175.

[18] Mead D.J., and Markus, S., Loss Factors and Resonant Frequencies of Encastré Damped Sandwich Beam, J Sound Vib, 1970;12(1):99-112.

[19] Rao, D.K., Frequency and Loss Factors of Sandwich Beams under Various Boundary Conditions, J Mech Eng Sci, 1978;20(5):271-282.

[20] López-Aenlle, M., Pelayo, F., Frequency Response of Laminated Glass Elements: Analytical Modelling and Effective Thickness, Appl Mech Rev, 2013;65(2), 020802 (13 pages).

[21] Wang, C.M., Vibration Frequencies of Simply Supported Polygonal Sandwich Plates via Kirchhoff Solutions. J Sound Vib, 1996;190(2):255-260.

[22] Nashif, A.D., Jones, D.I.G., and Henderson, J.P., Vibration Damping. John Willey and Sons, New York. 1985.

[23] Mead, D.J., The damping properties of elastically supported sandwich plates. Journal of sound and vibration. 24(3), 275-295, 1972.

[24] Mead, D.J., Yaman, Y. The harmonic response of rectangular sandwich plates with multiple stiffening: A flexural wave analysis. Journal of Sound and Vibration, 145(3), 409-428, 1991.

[25] M. López-Aenlle, F. Pelayo, Dynamic effective thickness in laminated-glass beams and plates. Composite: Part B, 67, 332-347, 2014.

[26] Pelayo, F. López-Aenlle M. Natural frequencies and damping ratios of multi-layered laminated glass beams using a dynamic effective thickness. Journal of sandwich structures and materials (10.1177/1099636217695479), 2017.

[27] Galuppi, L., and Royer-Carfagni, G.F., The Effective Thickness of Laminated Glass Plates, J Mech Mater Structures, 2012;7(4):375-400.

[28] Blevins, R.D., Formulas for natural Frequency and Mode Shapes, Krieger Publishing Company, Malabar, Florida, 2001.

[29] Brincker, R., Ventura, C. Introduction to Operational Modal Analysis. Wiley, 2015.

[30] Pelayo, F., López-Aenlle, M., Brincker, R. and Fernández-Canteli, A., Artificial Excitation in Operational Modal Analysis, In Proc. Of the 3th International Operational Modal Analysis Conference (IOMAC). Portonovo, Ancona. 2009, Paper 223.

[31] López-Aenlle, M., Pelayo, F., Fernández-Canteli, A., García Prieto, M. The effective-thickness concept in laminated-glass elements under static loading. Eng Struct, 2013;56:1092-1102.

[32] Ewins, D.J., Modal testing: theory, practice and application. Second Ed. Research Studies Press, LTD. John Willey and Sons, LTD. England, 2000.

FIGURE CAPTIONS

Figure 1. Section of a sandwich (a) and a multi-layered (b) glass beam.

Figure 2. Multilayered glass plate under simply supported conditions.

Figure 3. Accelerometers (arrows) Set-up used in the OMA test.

Figure 4. Singular value decomposition of the responses

Figure 5. Effect of decimation in the damping estimation for the first mode.

Figure 6. Experimental Set-up for the static test.

Figure 7. Displacement of the central point of the plate (Position A)

Figure 8. Displacement of the border mid-point (Position B).